122. Katayoun Sohrabi et al., A self organizing wireless sensor network, *Proc. 37th Annu. Allerton Conf. on Communication, Control, and Computing,* 1999, pp. 1201–1210.
123. Gregory J. Pottie, Wireless sensor networks, *Information Theory Workshop,* 1998, pp. 139–140.
124. http://bwrc.eecs.berkeley.edu.
125. Jan M. Rabaey et al., PicoRadio supports ad hoc ultra-low power wireless networking, *IEEE Computer,* v. 33, n. 7, July 2000, pp. 42–48.
126. Lizhi Charlie Zhong et al., An ultra-low power and distributed access protocol for broadband wireless sensor networks, presented at *Networld+Interop: IEEE Broadband Wireless Summit,* Las Vegas, 2001. http://bwrc.eecs.berkeley.edu.
127. Ibid.
128. http://robotics.eecs.berkeley.edu.
129. J. M. Kahn, R. H. Katz, and K. S. J. Pister, Next century challenges: mobile networking for Smart Dust, *Proc. Fifth Annual ACM/IEEE Int. Conf. on Mobile Computing and Networking,* 1999, pp. 271–278.
130. Brett A. Warneke et al., Smart dust: communicating with a cubic-millimeter computer, *Computer,* v. 34, n. 1, January 2001, pp. 44–51.
131. Brett A. Warneke et al., An autonomous 16 mm^3 solar-powered node for distributed wireless sensor networks, *Proc. IEEE Sensors,* 2002, v. 2, pp. 1510–1515.
132. http://www-mtl.mit.edu.
133. W. R. Heinzelman, A. Chandrakasan, and H. Balakrishnan, Energy-efficient communication protocol for wireless microsensor networks, *Proc. 33rd Annu. Hawaii Int. Conf. on System Sciences,* 2000, pp. 3005–3014.
134. http://www.terminodes.org.
135. http://www.ietf.org.
136. Jean-Pierre Hubaux et al., Toward self-organized mobile ad hoc networks: the Terminodes project, *IEEE Commun.,* v. 39, n. 1, January 2001, pp. 118–124.
137. M. Scott Corson, Joseph P. Macker, and Gregory H. Cirincione, Internet-based ad hoc networking, *IEEE Internet Computing,* v. 3, n. 4, July–August 1999, pp. 63–70.
138. Ibid.
139. Bertrand Baud, A communication protocol for acoustic ad hoc networks of autonomous underwater vehicles, Master's Thesis, 2001, Florida Atlantic University, Boca Raton, FL.
140. Ethem M. Sozer, Milica Stojanovic, and John G. Proakis, Underwater acoustic networks, *IEEE J. Oceanic Eng.,* v. 25, n. 1, January 2000, pp. 72–83.
141. John G. Proakis et al., Shallow water acoustic networks, *IEEE Commun.,* v. 39, n. 11, November 2001, pp. 114–119.
142. Ibid.
143. Clare, Pottie, and Agre, ibid.
144. J. Agre and L. Clare, An integrated architecture for cooperative sensing networks, *Computer,* v. 33, n. 5, May 2000, pp. 106–108.

Chapter 3
The Physical Layer

3.1 INTRODUCTION

This chapter describes a physical layer for wireless sensor networks. A unique Direct Sequence Spread Spectrum (DSSS) modulation method is described and evaluated that enables a high data rate, which is desirable to minimize total transceiver active time and, therefore, maximize battery life, while minimizing transceiver complexity. Performance is simulated in Additive White Gaussian Noise (AWGN) and a Bluetooth™ interference environment.

A communication protocol physical layer

> *... provides mechanical, electrical, functional, and procedural characteristics to establish, maintain, and release physical connections (e.g., data circuits) between data link entities.*[1]

Wireless sensor networks are designed to handle very low data throughput (as low as a few bits/day), exchanging lower throughput and higher message latency for longer node battery life, lower cost, and self-organization. Target applications for these networks are inventory management, industrial control and monitoring, security, intelligent agriculture, and consumer products such as wireless keyboards and personal computer (PC)-enhanced toys. The networks often have stringent cost and battery life goals; nodes in an Institute of Electrical and Electronics Engineers (IEEE) 802.15.4 Low-Rate Wireless Personal Area Network (LR-WPAN), for example, must have multiyear operation from a 750 mAh AAA cell while being considerably simpler (having fewer logic gates, smaller analog circuitry, and less memory) than a comparable Bluetooth device. In addition, the system must be capable of universal (worldwide) unlicensed operation, which greatly limits possible frequency band, modulation, and other physical layer alternatives.

Because the major design metrics of a wireless sensor network are its cost and power consumption, the physical layer design of a wireless sensor network is critical to its success.[2] Unfortunate choices of modulation, frequency band of operation, and coding can produce a network that, although functional, does not meet the cost or battery life goals needed for market acceptance. Although one-way networks have been proposed (in which sensors transmit to a central receiver) to achieve low cost and low

power consumption,[3] this work will consider only two-way networks, in which all network nodes may both transmit and receive. Further, the networks will be capable of multi-hop operation to reduce overall network power consumption.[4,5]

3.2 SOME PHYSICAL LAYER EXAMPLES

Although wireless sensor networks may be conceived to communicate via many different mechanisms, including both electromagnetic (both radio frequency (RF) and infrared) and audio means, this chapter will focus on an RF physical layer. A survey of some relevant RF physical layers includes the following subsections.

3.2.1 BLUETOOTH

Bluetooth, a WPAN, operates in the 2.4 GHz Industrial, Scientific, and Medical (ISM) band. It employs binary Gaussian Frequency Shift Keying (GFSK), with a symbol rate of 1 MBaud. At the time of its development, devices in the 2.4 GHz ISM band were required by regulation in many countries to employ spread spectrum techniques. Bluetooth performs frequency hopping spread spectrum, randomly hopping across 79, 1-MHz channels (in the United States) at a rate of 1600 hops per second.[6,7]

Although Bluetooth is often suggested for sensor network applications, the Bluetooth physical layer is not very suitable for wireless sensor networks. Frequency hopping spread spectrum makes network discovery and association difficult because the network and prospective member node are asynchronous and the search must be done on a packet rate time scale. This causes a power consumption problem as the prospective member searches the band for the network, which may, in fact, not be present, and is especially problematic for low duty rate systems. Further, frequency hopping systems employ relatively narrowband modulation schemes (1 MHz wide in the case of Bluetooth); this means that integrated channel filtering will be difficult and expensive due to the large component (usually capacitor) values required to achieve the low-frequency filter corner. In addition, the large capacitor values associated with low-frequency circuits must be charged to a bias voltage during circuit warm-up, prior to operation; this lengthened warm-up period negatively affects node duty cycle. Further, the narrow channel separation makes the phase noise requirements of signal sources in both transmitter and receiver more difficult.

3.2.2 IEEE 802.11b

The IEEE 802.11b WLAN standard also specifies operation in the 2.4 GHz ISM band. Although similar, regulations for the 2.4 GHz band are not the same around the world:

The standard provides for 14 overlapping channels of 22 MHz between 2.4 and 2.5 GHz. Not all channels are usable in all regulatory areas; e.g., only channels 1 through 11 may be used in the United States. Channel centers are spaced 5 MHz apart.[8]

As noted in Chapter 2, the original 802.11 standard specified three physical layer options at 1 Mb/s (with an optional 2 Mb/s) — infrared as well as both frequency hopping and direct sequence spread spectrum in the 2.4 GHz band. The direct sequence layer, operating at a chip rate of 11 Mc/s, employed differential binary phase shift keying (DBPSK) at 1 Mb/s, and differential quadrature phase shift keying (DQPSK) at 2 Mb/s; 802.11b extends the direct sequence layer to 5.5 and 11 Mb/s by a technique called complementary code keying (CCK). In CCK, the chip rate and modulation type remain the same as for the 2 Mb/s rate — 1 Mc/s and DQPSK, respectively — but additional information is placed in each symbol by selecting different spreading codes. For the 5.5 Mb/s rate, four possible spreading codes can be used, so two bits of information can be placed in the DQPSK modulation, and two bits of information can be placed by choice of spreading code, for a total of four bits per transmitted symbol. For the 11 Mb/s rate, 64 spreading codes are possible, so a total of 8 bits (1 byte) may be transmitted per symbol. The standard provides for an alternative, optional technique, packet binary convolutional coding (PBCC), which produces the same 5.5 and 11 Mb/s data rate as CCK but with improved sensitivity, at the cost of increased receiver complexity.[9]

The original 1- and 2-MHz direct sequence 802.11 physical layer is a possible candidate for a wireless sensor network; its hardware requirements are simple, the data rate is high enough, and the use of direct sequence means that it avoids the problems of frequency hopping systems. However, the use of an 11-Mc/s chip rate is somewhat onerous for a low power device; it would be desirable to operate circuits associated with the pseudonoise (PN) chip sequence at a lower rate. The cost and power consumption of the extended 802.11b systems, on the other hand, are far beyond that feasible for wireless sensor networks; for example, the large number of correlators needed to identify and decode the CCK chip sequences would be far too large, and dissipate far too much power, for the receiver of a wireless sensor node.[10]

3.2.3 Wireless Sensor Networks

Many studies of wireless sensor networks have not defined the physical layer and have used existing wireless components for their first demonstration networks. However, some investigators have considered the physical layer.

3.2.3.1 PicoRadio. Rabaey et al.[11] find ultrawide band systems attractive for the physical layer of wireless sensor networks because ease of integration (i.e., low cost) is of higher priority than bandwidth efficiency. An interesting feature of the PicoRadio physical layer is the proposed use of "wake-up radios," namely:

> *To support sleep mode, a wakeup radio is used in the physical layer, which consumes less than 1 μW running at full duty cycle. It wakes up the main radio and informs it of the channel it should tune to. Because the destination ID is modulated into the wakeup signal, only the destination node will be waken [sic] up.*[12]

This concept had also been considered in the Piconet program of the University of Cambridge (England) and the Olivetti and Oracle Research Laboratory,[13] Cambridge, England, since renamed the Prototype Embedded Network (PEN) program.[14–16] (The PEN program was discontinued in 2002.) The wakeup receiver provides low average power consumption without the strict internode timing synchronization that would otherwise be necessary because only short pulses of the high power consumption ultrawide band receiver would be possible.[17]

3.2.3.2 WINS. The WINS system employs spread spectrum signaling, in either the 900 MHz or 2.4 GHz ISM bands. The physical layer design is "directed to CMOS circuit technology to permit low cost fabrication along with the additional WINS components."[18]

3.2.3.3 μAMPS. Wang et al.[19] and Shih et al.[20] note the importance of multilevel signaling to minimize the time a network node is actively communicating and, therefore, maximize the time it is sleeping (and thereby conserving power). Further, they identify the problem of start-up energy, which is the energy taken by a wireless transceiver during its transition between the sleep and active modes, and note that the energy consumed during start-up may be greater than that consumed during active operation. This occurs because the transmission time may be very short, but the start-up time is limited by physical time constants inherent in the physical layer implementation.

3.3 A PRACTICAL PHYSICAL LAYER FOR WIRELESS SENSOR NETWORKS

This section concerns the design of a physical layer suitable for wireless sensor networks. Because the primary metrics of wireless sensor protocol design are cost and battery life, it is instructional to consider each in detail.

3.3.1 Cost

The physical layer's effect on network cost is largely due to the cost of hardware — the cost of chip(s) and external parts. Integration typically reduces

cost because fewer discrete parts must be purchased, handled, and placed in the final product; in the limit, one may consider a single-chip design with only an antenna and a battery as external parts (the integration of antennas[21] and batteries[22–24] will be substantially more difficult, although not impossible). Aside from the antenna and battery, the most difficult component to integrate may be the quartz crystal frequency reference. A promising alternative to the discrete quartz crystal is the integrated microelectromechanical system (MEMS) resonator.[25] One consideration in the design of the physical layer is the required reference frequency stability. Although quartz crystal resonators routinely achieve less than five ppm (pages per minute) frequency variation over consumer temperature ranges, they are a mature technology; first- or second-generation MEMS resonators may not be capable of such stability, and the physical layer design should not require it.

Another consideration for low-cost integrated devices is the relative amounts of analog and digital circuitry required. As is well known, digital circuits dimensionally shrink with lithographic improvements in integrated circuit processing; analog circuits, however, generally do not shrink with process improvements. Not only are the dimensions of analog transistors controlled by factors other than process capability (such as current density), they also often employ passive components, the dimensions of which are controlled by physical factors such as capacitor dielectric constant. Therefore, as process technology advances, digital circuits become smaller and, therefore, cheaper, while the size of analog circuits remains relatively unchanged. Further, as integrated circuit technology advances and minimum feature size is reduced, the cost of die area actually increases. This penalizes analog circuits, which become more expensive with process improvements.

The lowest cost implementation, therefore, is either (1) a nearly all-analog approach in a large-dimension, relatively old process with a low cost per die area, or (2) a nearly all-digital approach in a small-dimension, state-of-the-art process with a low cost per digital gate. The deciding factor is that the desired system-on-a-chip (SoC) design must include RF circuits, as well. These likely cannot be made in a large-dimension process, due to the lower gain-bandwidth product of the transistors. The nearly all-digital approach is, therefore, the proper approach.

Note that the digital approach is the proper approach even if, at a given point in integrated circuit process development, the total circuit area of the digital-centric approach is larger than an alternative analog-centric approach. With process improvements over time, the cost of the digital approach will monotonically drop, while the cost of the analog approach will, at best, remain constant (if one stays with an aging process) or may even increase (if the integrated circuit (IC) vendor no longer supports the old process and the design must be moved to a more modern one).

One of the largest circuits in many transceivers is the channel filtering of the receiver. The channel filters, if analog, are typically large because the filters require relatively large capacitors to obtain sufficient strong signal (dynamic range) performance;[26] even if the main channel filtering is done with a digital filter, after an analog-to-digital converter, the analog-to-digital converter requires an antialias filter before it. The size of the analog channel filter is inversely proportional to the filter's corner frequency; if possible, the physical layer design should maximize the required channel filtering corner frequency (i.e., have a wide bandwidth) to minimize the die area, and therefore the cost, of the resulting IC. In addition, the amount of channel selectivity required in the physical layer should be as little as possible, consistent with proper network operation, so that as few poles of filtering as possible may be specified.

Another factor in network cost that is affected by the physical layer is the need to maximize market size and, therefore, achieve cost reductions due to volume production. This means that the physical layer should be compatible with the regulations in as many countries worldwide as possible. The first decision is the frequency band in which to operate. Clearly, it is impractical to license individual wireless sensor network nodes, or even the actual networks, just due to their expected ubiquity and low maintenance and cost goals. This then requires the identification of a band, available nearly worldwide, that allows unlicensed operation and has sufficient bandwidth. The bands that meet these requirements are the unlicensed ISM bands.

An additional requirement is the ability to integrate, with available or soon-to-be-available technology, a radio transceiver for the chosen band in the network node SoC.[27,28] Although operation as high as 60 GHz has been proposed for some consumer products,[29] and future integration of a 60-GHz transceiver with SoC-compatible technologies (e.g., silicon CMOS) does not seem out of the question,[30] at present 60-GHz operation requires "exotic" materials (e.g., compound semiconductors, such as gallium arsenide) that make a SoC design impractical due to cost and current drain considerations. Node operation at relatively low frequencies, below 1 GHz, suffers from the poor efficiency of electrically small antennas because the physical size of network nodes is limited.[31] Choice of the proper ISM band is, therefore, a compromise between the cost and power drain associated with high-frequency operation, and the physical size and antenna efficiency limitations associated with low-frequency operation. Above 1 GHz and below 60 GHz, three ISM bands are used: the 2.4-GHz band (2.400–2.4835 GHz in the United States); the 5.8-GHz band (5.725–5.875 GHz in the United States);[32] and the 24-GHz band (24.000–24.250 GHz in the United States). Of these, the 2.4-GHz band was chosen as having the best combination of antenna efficiency and power consumption.

Note that the 2.4-GHz band is not unoccupied; similar to all ISM bands, it is populated with many services. The IEEE 802.11b (Wi-Fi™) WLAN and the Bluetooth WPAN, among a host of other services, are in the 2.4-GHz band. The study of how these services coexist is, therefore, of significant interest, and must be considered in the evaluation of the proposed wireless sensor network physical layer.[33,34] As discussed in this chapter and in Section 4.3.4 of Chapter 4, a complicating factor in unlicensed bands (beyond the simple reduction of data throughput caused by packet collisions and retransmissions) is that different services often employ different channel access mechanisms; this situation can result in unfair channel access to one service over another. These problems can be mitigated to a degree by a physical layer design that is resistant to the interference environment (e.g., by using spread spectrum techniques to provide processing gain).

An alternative that has recently become available is the use of the 3.1–10.6 GHz ultrawideband (UWB) frequency band, defined by the Federal Communications Commission (FCC).[35] The use of UWB techniques instead of conventional carrier-based modulation schemes can offer improved location determination performance (down to the centimeter range), can support very high network node densities, and can have a very low probability of detection — all critical factors for some wireless sensor network applications. Although much of the world may follow the lead of the FCC and establish similar regulations (perhaps after a period of cautious observation of the new technology), at present, such a physical layer would be limited to the United States.

3.3.2 Power

Two aspects of the power problem must be considered in the physical layer design: the behavior of the power source and the power consumption of the system.

3.3.2.1 Power Source. Because the average power consumption of a wireless sensor network node is expected to be very low, on the order of 50 μW or less, unconventional power sources become plausible alternatives. These include those based on scavenging from ambient sources of energy, such as solar, RF, and mechanical vibration sources.[36,37] However, despite their usefulness in particular applications, each of these sources has limitations — solar-powered devices must be lit, and vibration-powered devices, of course, must have vibration. To maintain generality, this chapter considers the more conventional battery.

Although many battery technology alternatives are available, and many criteria exist for the selection of a battery technology for a specific application,[38] the design of a protocol physical layer can take advantage of a critical behavior of batteries that seems to be technology independent. A bat-

tery undergoing pulsed discharge has a greater capacity than an identical battery undergoing a constant discharge. Further, the lower the duty cycle of the pulsed discharge, the greater the battery capacity. This charge recovery effect has been demonstrated experimentally in manganese–zinc, alkaline–manganese,[39] and lead–acid[40] cells, modeled and demonstrated experimentally in manganese–zinc[41] and lithium–ion[42] cells, and modeled in zinc–zinc oxide cells;[42] it has even been modeled in more esoteric battery technologies, such as the lithium–aluminum, iron sulfide battery.[43]

Use of the charge recovery effect has been proposed as a method of extending the battery life of portable communication devices;[45–48] its use in the physical layer of wireless sensor networks, which have low duty cycle, bursty communication, is a clear opportunity. In practice, taking advantage of the charge recovery effect means that the protocol should activate high-power dissipation components (e.g., the transceiver) in infrequent bursts (resulting in a low duty cycle of operation). Also, the bursts should be separated from each other by the maximum extent possible, thereby giving the cell the maximum possible time to recover before the next discharge pulse.

3.3.2.2 Power Consumption. Because the active power consumption of the transceiver in a wireless sensor network node is much greater than its standby power consumption, the node must operate its transceiver in a low duty cycle mode to get low average power consumption. One is then placed in the happy position in which the operating condition of the node that provides the lowest average power drain is exactly the condition that maximizes the available battery capacity.

A typical 2.4-GHz CMOS transceiver of modest specification and power output (e.g., 0 dBm) will have a power drain of about 32 mW while transmitting and about 38 mW while receiving (taking the values from Appendix C[49] and adding 5 mW for microcomputer power consumption). For the purpose of a duty cycle calculation in a peer-to-peer network, one may make the simplifying approximation that the power drains of both transmitter and receiver are the same (an average of 35 mW), and the further simplifying assumption that the communication links are symmetrical (that is to say, equal time is spent transmitting and receiving). To meet a 1-year battery life goal with such a transceiver under these assumptions, its duty cycle must be extremely low: if we assume a battery life goal of one year (8760 hours) from two, 750-mAh AAA cells in series, an average current drain of

$$I_{avg} = 750 \text{ mAh}/8760 \text{ h} = 86 \text{ μA} \quad (1)$$

is required. If the node transceiver is supplied from these batteries through a 1.8 V linear voltage regulator, in which the output current equals the input current, an average power drain

$$P_{avg} = 1.8 \text{ V} * 86 \text{ μA} = 154.8 \text{ μW} \quad (2)$$

is required. For this system, the average current drain is

$$I_{avg} = T_{on} * I_{on} + (1 - T_{on}) * I_{stby} \quad (3)$$

where

T_{on} = Fraction of time either receiver or transmitter is on
I_{on} = Current drain from the battery when either the receiver or transmitter is on
I_{stby} = Current drain from the battery when both transmitter and receiver are off

From this equation, and estimates of the current consumption of practical hardware, the maximum acceptable T_{on} may be determined as a function of the maximum device average battery current. For example, if I_{on} = 19.5 mA, I_{stby} = 30 μA, and I_{avg} = 86 μA, T_{on} = 0.0029, or 0.29 percent. This low value implies that, despite the low data throughput of wireless sensor networks, a relatively high data rate is required so that an active device may finish communication quickly and return to sleep, to produce the low duty cycle needed to meet the system battery life requirements. This must be achieved, of course, without increasing I_{on} excessively.

Active power consumption of a transceiver is more closely tied to the symbol rate than to the raw data rate. Although it is desirable to maximize the raw data rate to minimize power consumption (by minimizing T_{on}), it is, therefore, also desirable to minimize the symbol rate, to minimize I_{on}. The simultaneous requirements of maximizing data rate and minimizing symbol rate leads one to the conclusion that multilevel or *M-ary* signaling (i.e., sending more than one bit per symbol) should be employed in the physical layer of wireless sensor networks.[50,51] The use of *M-ary* signaling, however, cannot be done indiscriminately; for example, if simple multiple phase *M-ary* signaling were used, the result would be a reduction of detection sensitivity that, to recover link margin, would require an increase in transmitted power that could result in no net power consumption savings. To avoid this, some type of orthogonal *M-ary* signaling should be employed.[52]

The value of T_{on} includes any warm-up time of the communication circuits, during which no communication is possible, but large amounts of current may be drawn from the battery. If the actual communication time is sufficiently small, the primary factor determining battery life may, in fact, be warmup current drain.[53,54] It is, therefore, important to minimize the length of the warmup time; the physical layer protocol may ease the

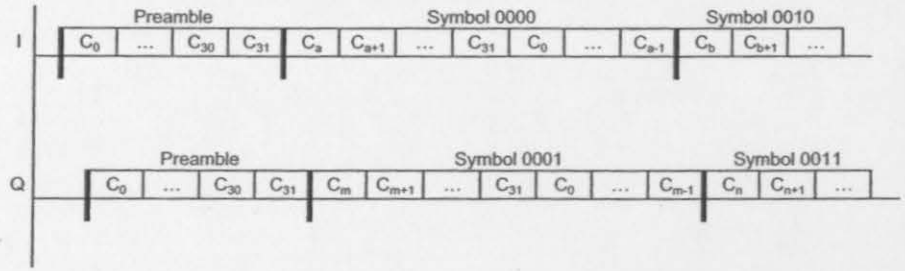

Exhibit 1. Code Position Modulation

task of the hardware designer by considering channel frequencies and spacing that allow a high synthesizer reference frequency to be used (for fast lock time) and reducing or eliminating requirements for narrow bandwidth filtering (for example, in channel selectivity filters). This gives wide bandwidth systems, such as direct sequence spread spectrum systems, an advantage over narrowband systems for low duty cycle networks.[55] To minimize I_{on}, however, it is important to minimize the chip rate of the direct sequence system, just as the symbol rate should be minimized.

An additional advantage of direct sequence systems is that their implementations have a high digital circuit content, and relatively low analog circuit content. As noted earlier, this is desirable for cost reasons due to the economics of integrated circuit fabrication.

Although the rules have recently been modified in the United States,[56–58] in many other parts of the world, operation in the 2.4-GHz band requires some form of spread spectrum modulation if a significant amount of transmitted power is to be employed. (Lower-power classes of operation that do not require spreading are used in most countries.) Further, the European regulations allow a higher transmit power, which may be desired in certain applications if the raw data rate is at least 250 kb/s.[59] For these reasons, plus its cost and low power advantages, the proposed physical layer employs direct sequence spread spectrum modulation, with a raw data rate of 250 kb/s.

The modulation scheme used in this work is called differential code (or pulse) position modulation; it employs two 32-chip (augmented) random pseudonoise (PN) sequences, one each on the I and Q channels, transmitted with offset-quadrature phase shift keying (QPSK). Half-sinusoidal pulse shaping of the chips is employed; the resulting modulation then has a constant envelope[60] and is, therefore, suitable for inexpensive nonlinear power amplifiers. The PN sequences used are maximal-length sequences (m-

sequences). The I channel uses the PN sequence with the characteristic polynomial 45 (octal), and the Q channel uses the PN sequence with the characteristic polynomial 75 (octal).[61] The symbol rate is 31.25 kSymbols /s. As illustrated in Exhibit 1, information is placed on each channel in each symbol by cyclically shifting the PN sequence of each channel by one of 16 possible shift values.[62,63] The information is placed on each channel differentially (i.e., the information is the difference in shift values between that of the present symbol and the one immediately preceding it on the same channel). Because one of $M = 16$ shift values (each containing $k = 4$ bits of information) are placed on each of the I and Q channels during one symbol time, a total of eight bits (one byte) are transmitted per symbol. (Because 32 chips are in the PN sequence, it is possible to set $M = 32$ and send $k = 5$ bits in each symbol, but this was not done for reasons of complexity; it is easier to parse eight-bit bytes into four bits than five, and having fewer shift values simplifies receiver implementation.) Because the packet lengths will be short (< 100 bytes), symbol synchronization is achieved during a PHY packet preamble and fixed during data transmission.

Code position modulation is a form of orthogonal coding in which the symbols transmitted on each of the I and Q channels are selected from a set of orthogonal codewords, in this case each 32 chips long. For equally likely, equal-energy orthogonal signals, the probability of bit error $P_B(k)$ in a single I or Q channel can be bounded by[64]

$$P_B(k) \le (2^{k-1})Q\left(\sqrt{\frac{kE_b}{N_0}}\right) \tag{4}$$

where

$$Q(x) = \frac{1}{\sqrt{2\pi}}\int_x^\infty \exp\left(-\frac{u^2}{2}\right)du \tag{5}$$

is the complementary error function, k is the number of information bits sent in each symbol, E_b is the received signal energy/bit, and N_0 is the thermal noise power spectral density.[65] Because data is encoded differentially in the proposed modulation method, however, symbol errors occur in pairs; this doubles the bit error rate (BER):

$$P_B(k) \le (2^k)Q\left(\sqrt{\frac{kE_b}{N_0}}\right) \tag{6}$$

Orthogonal coding enjoys increased, instead of decreased, detection sensitivity over the uncoded binary waveform; that is, the value of E_b/N_0

required for a given bit error probability is lower for orthogonal coding than for the uncoded binary waveform. The cost is an increase in bandwidth; however, bandwidth efficiency is not a critical performance metric for wireless sensor networks, due to their low offered data throughput.

Code position modulation, by employing a single PN sequence per channel, offers significant cost savings over a conventional multilevel direct sequence system, by simplifying PN code generation. The conventional system requires that separate PN sequences be generated for each possible transmitted sequence and compared with the received sequence. Code position modulation allows the PN code to be generated once, compared with the received sequence, and then cyclically shifted and compared again. In many integrated circuit implementations, the generation and storage of PN sequences can represent a large portion of the die area, and, therefore, the cost, of the receiver. For the proposed system in which 16 possible sequences per channel may be sent, the reduction in die area enabled by generating one sequence per symbol, instead of 16, can be significant; because shifting a PN sequence is a lower-power activity than generating a PN sequence, power consumption is also lower.

The orthogonal signaling technique has been applied to high-speed physical layers (e.g., IEEE 802.11b[66]), but its application to wireless sensor networks is believed to be a novel approach.

3.4 SIMULATIONS AND RESULTS

This physical layer was simulated in version 4.5 of the Signal Processing Worksystem (SPW) from Cadence Design Systems, San Jose, California, to determine the detector sensitivity (E_b/N_0), and susceptibility to interference from Bluetooth transmissions, which may also be present in the 2.4-GHz band. SPW is described in Appendix A.

3.4.1 Simulations

As illustrated in Exhibit 2, the BER simulation is both simple and flexible. Both I and Q channels are generated and detected independently, so that studies of possible differences in performance between them (due to autocorrelation differences between PN sequences, for example) may be made. This results in some slowdown of simulations, but because the packet size in these systems is so small (< 800 bits), there is little need for BER information below BER = 10^{-5}. This means that the long simulations needed (to achieve a statistically significant number of bit errors) for lower BERs are unnecessary, so simulation speed is not of critical importance.

The modulator block (Exhibit 3) produces the desired shifted PN sequence, based on the incoming data, from the 16 possible choices. After combining the I and Q channels, the transmitted signal is sent over an

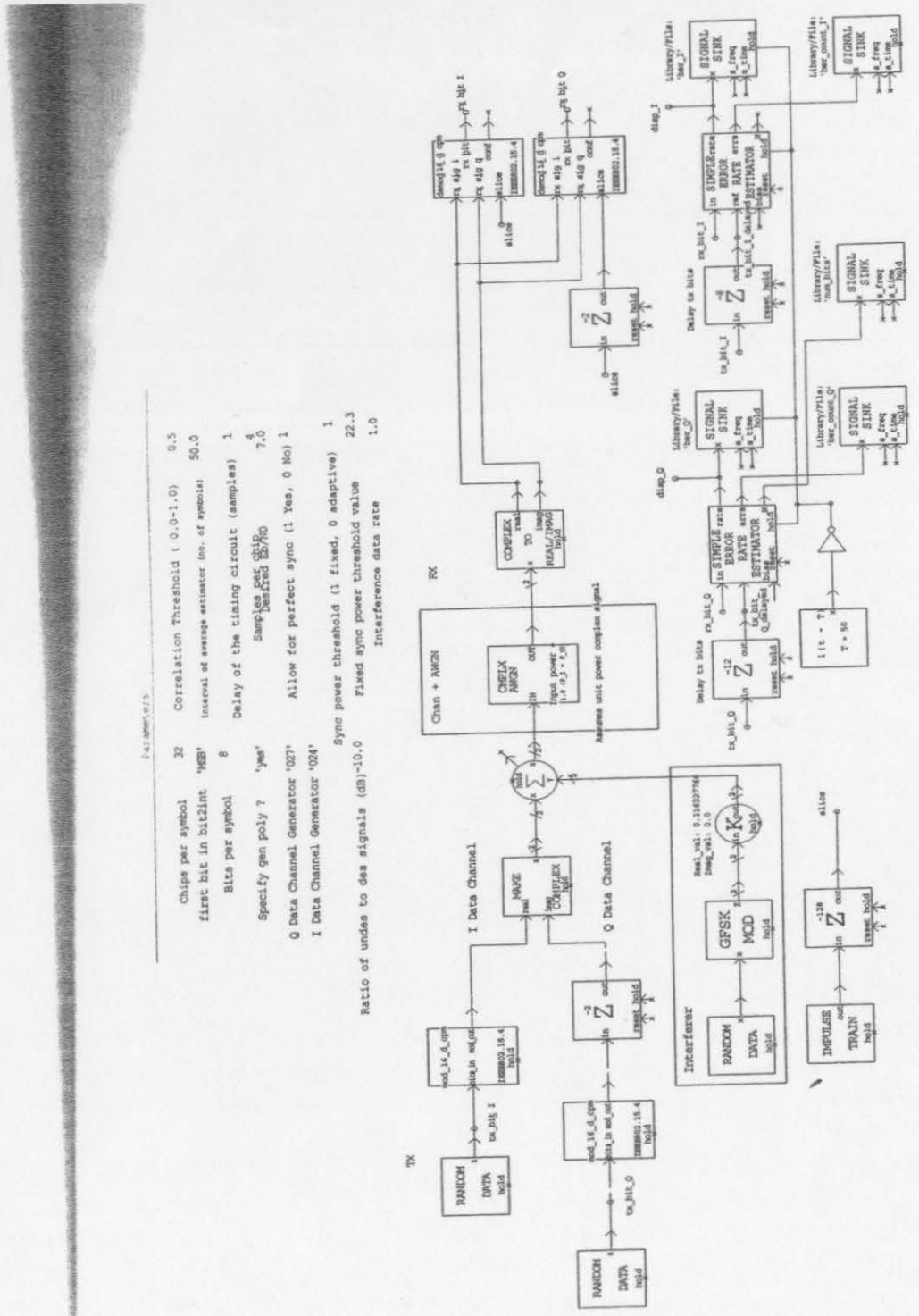

Exhibit 2. Code Position Modulation Simulation in SPW

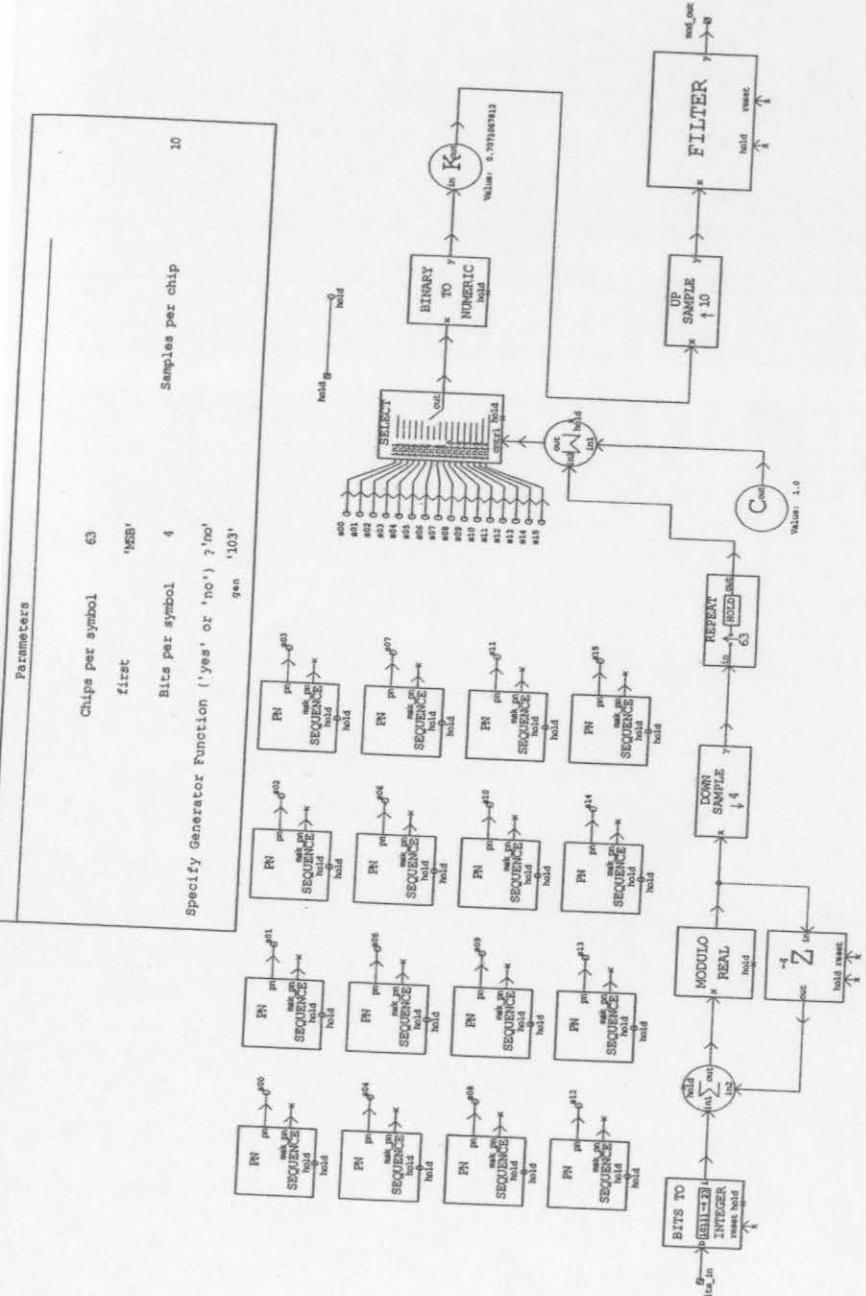

Exhibit 3. SPW Simulation of CPM Modulator

AWGN channel block representing receiver noise. This block is a large file of random noise, used so that repeatable results could be obtained even when modifications to the system were made.

The range of a wireless sensor network communication link is usually limited by design to 10 meters or less, so the one-way flight delay of the RF signal, even if via an indirect (e.g., reflected) path, is 30 nanoseconds or less. Because the duration of a chip is one microsecond, the effects of multipath interference were not considered significant and so were not simulated.

The demodulator block (Exhibit 4) is a correlator to each of the 16 possible transmitted sequences on each channel, matched to the half-sine-shaped chips. Because the purpose of this study was to investigate the performance of the proposed physical layer during data transmission, instead of the performance of potential symbol synchronization algorithms, the symbol synchronization was fixed (i.e., "hard-wired" from transmitter to receiver).

To investigate the effects of potential interference from Bluetooth devices, which will also occupy the 2.4-GHz ISM band, a Bluetooth interfering scenario was simulated (Exhibit 5).

The Gaussian minimum shift keying (GMSK) modulator block in the SPW communication library was modified to reduce its modulation index from 0.5 to 0.315, the nominal Bluetooth value. An adjustable gain block was placed after the GFSK modulator, to control the ratio of undesired to desired signal level. The GFSK modulator was fed with 1-Mb/s random data, and no attempt was made to offset or randomize the phases of the 1-Mb/s Bluetooth data bits and the 1-Mc/s direct sequence chips. Similarly, no attempt was made to model any higher-protocol stack levels (e.g., frame structure) of either Bluetooth or the sensor network, so neither packet error rate (PER) nor message error rate (MER) was simulated.

3.4.2 Results

The BER versus E_b/N_0 performance of the proposed modulation method, as simulated by SPW, is given in Exhibit 6, and is compared with the theoretical prediction of Equation 5 for $k = 1$ and $k = 4$. The SPW Grouping parameter script was run to link the number of samples simulated with the E_c/N_0 parameter (and, therefore, the expected number of bit errors), so that each data point was simulated just long enough to obtain 100 bit errors. This minimized simulation time while ensuring statistically valid results. The E_b/N_0 ratio, required in this simulation to achieve 1 percent BER using the proposed modulation method, is approximately 5.2 dB. This is within 1.25 dB of the theoretical value calculated using Equation 5 with $k = 4$, and is approxi-

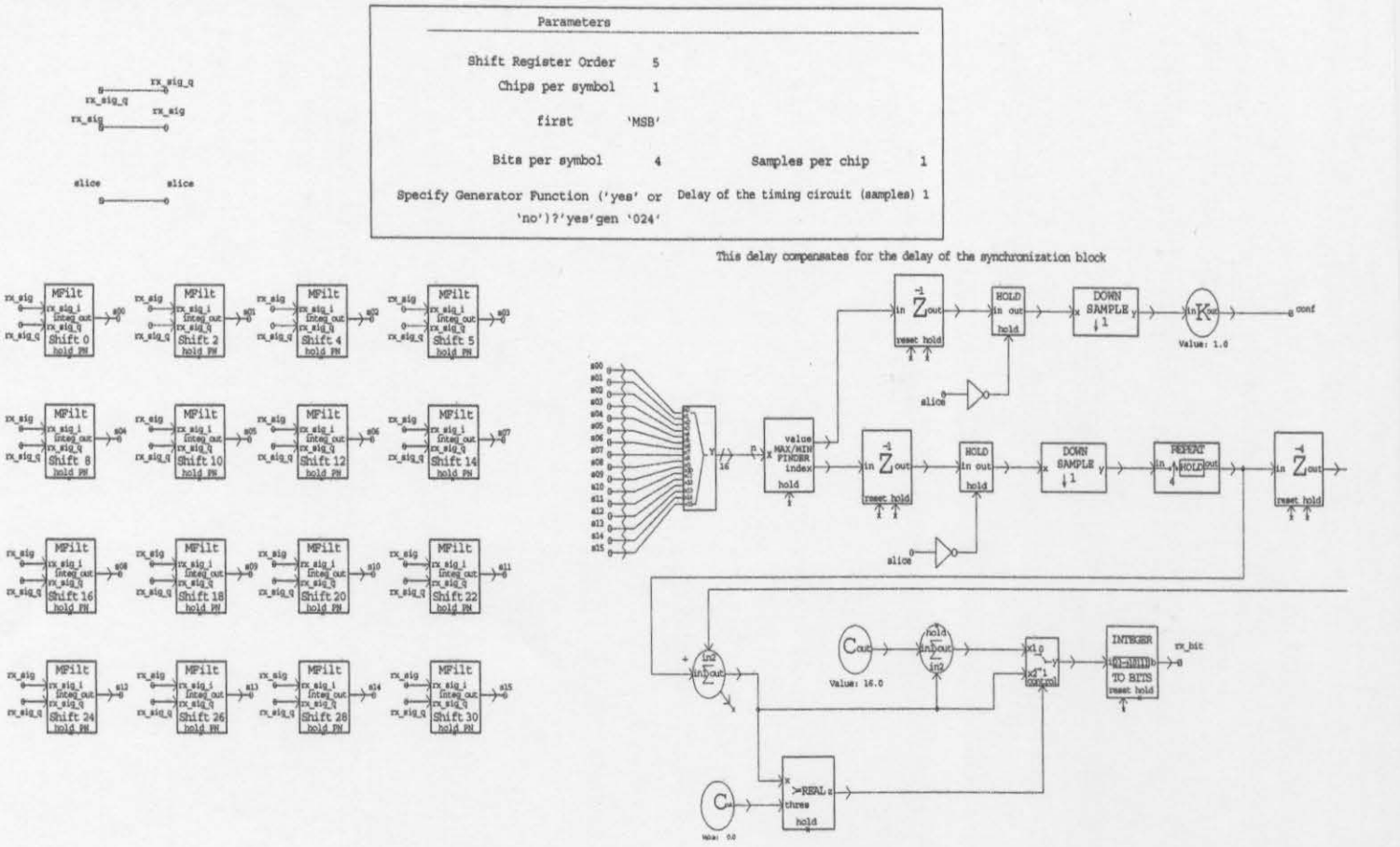

Exhibit 4. SPW Simulation of CPM Demodulator

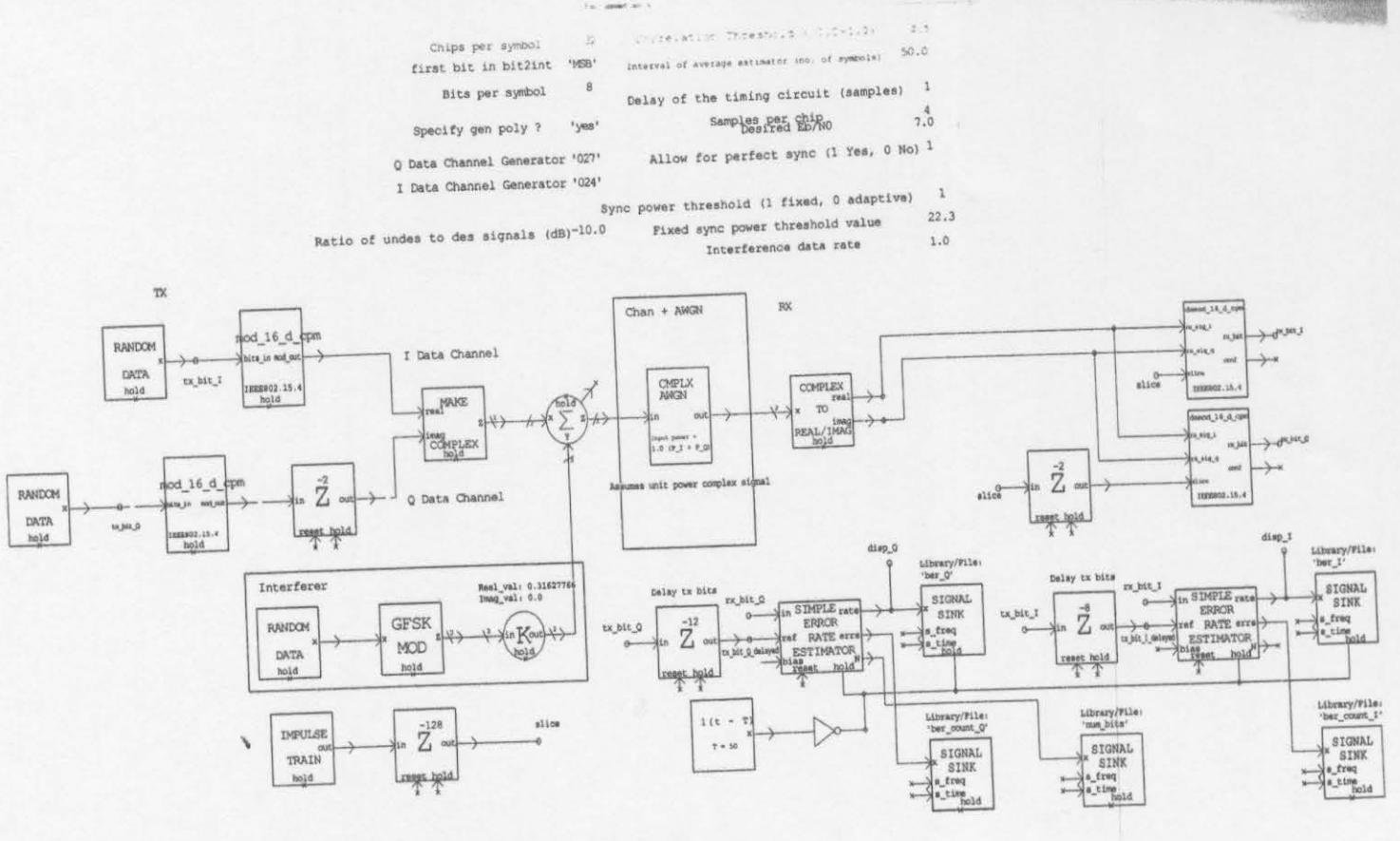

Exhibit 5. SPW Simulation of Bluetooth Interference Scenario

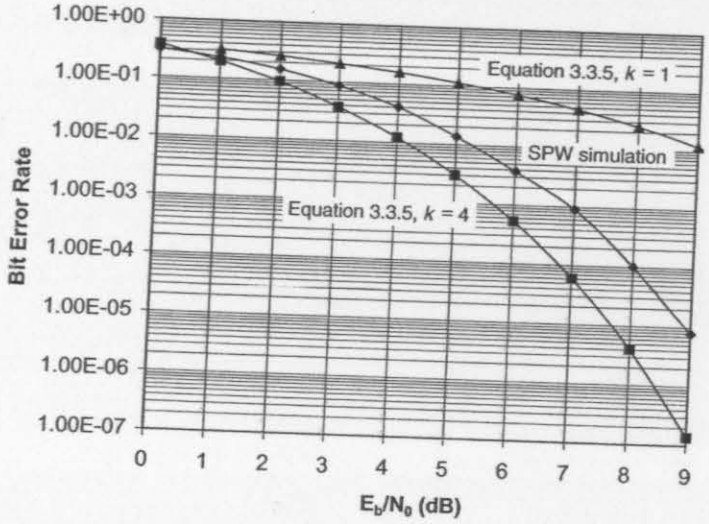

Exhibit 6. BER Performance of Code Position Modulation versus E_b/N_0

mately 4 dB better than that obtained with $k = 1$ (i.e., binary orthogonal signaling).

The 1.25-dB difference between the simulation results and Equation 5 is largely due to the nonideal autocorrelation and cross-correlation properties of the PN sequences chosen for the I and Q codes. The correlation between a code and, itself shifted in time, is close to, but not exactly, zero; similarly, the correlation between the 45 (octal) code on the I channel and the 75 (octal) code on the Q channel is not zero. This means that the signals used are not precisely orthogonal, as assumed by the theory; this trade of sensitivity was made in exchange for the simple circuit implementation that results.

The effect of Bluetooth interference on the sensor network BER was also simulated. The scenarios simulated were interference to a relatively weak sensor network signal, with an E_b/N_0 level of 4 dB, a somewhat stronger sensor network signal, with an E_b/N_0 level of 7 dB, and a very strong sensor network signal, with an E_b/N_0 level of 50 dB. The amount of Bluetooth interference was parameterized and allowed to vary in amplitude relative to the desired signal level, from –10 to +15 dB. The results, presented in Exhibit 7, demonstrate clearly the effect of spread-spectrum processing gain, and the ability of the system to survive, albeit at an increased BER, even in the presence of interfering Bluetooth signals stronger than the desired sensor network signal.

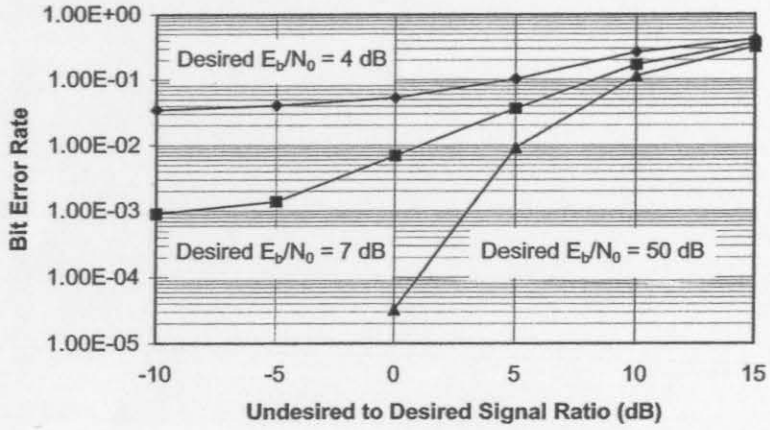

Exhibit 7. BER Performance of Code Position Modulation in the Presence of Bluetooth Interference

3.5 CONCLUSION

Features required to meet the cost and power consumption requirements of a wireless sensor network physical layer were reviewed, including the need to support high levels of integration and low duty cycle operation. Code position modulation, a type of modulation not previously proposed for wireless sensor networks, was shown to be compatible with these features. This modulation method enables a relatively high data rate, which is needed to reduce device duty cycle and thus improve battery life. This method is also compatible with a high level of digital, as opposed to analog, integration and, therefore, can enable low-cost implementations. The BER versus E_b/N_0 performance of code position modulation was simulated with SPW, and good agreement was found between the simulation result and that predicted by analytical theory. Because the network will operate in the 2.4-GHz band, and may experience interference from Bluetooth devices, a second simulation was performed to evaluate the BER in the presence of varying levels of Bluetooth interference. The expected resistance to narrowband signals caused by the processing gain of the spread spectrum modulation was observed in the simulation.

References

1. Hubert Zimmermann, OSI reference model — the ISO model of architecture for Open Systems Interconnection, *IEEE Trans. Commun.*, v. COM-28, n. 4, April 1980, pp. 425–432.
2. A. A. Abidi, Gregory J. Pottie, and William J. Kaiser, Power-conscious design of wireless circuits and systems, *Proc. IEEE*, v. 88, n. 10, October 2000, pp. 1528–1545.

3. Carl Huben, The Poisson network, *Circuit Cellar,* n. 113, December 1999, pp. 12–19.
4. I. Stojmenovic and Xu Lin, Power-aware localized routing in wireless networks, *IEEE Trans. Parallel and Distributed Syst.,* v. 12, n. 11, November 2001, pp. 1122–1133.
5. Priscilla Chen, Bob O'Dea, and Ed Callaway, Energy efficient system design with optimum transmission range for wireless ad hoc networks, *Proc. IEEE Intl. Conf. Commun.,* 2002, v. 2, pp. 945–952.
6. Jaap C. Haartsen and Sven Mattisson, Bluetooth — a new low-power radio interface providing short-range connectivity, *Proc. IEEE,* v. 88, n. 10, October 2000, pp. 1651–1661.
7. Tom Siep, *An IEEE Guide: How to Find What You Need in the Bluetooth Spec.* New York: IEEE Press. 2001.
8. Roger B. Marks, Ian C. Gifford, and Bob O'Hara, Standards in IEEE 802 unleash the wireless Internet, *IEEE Microwave,* v. 2, n. 2, June 2001, pp. 46–56.
9. Chris Heegard et al., High-performance wireless ethernet, *IEEE Commun.,* v. 39, n. 11, November 2001, pp. 64–73.
10. Brent A. Myers et al., Design considerations for minimal-power wireless spread spectrum circuits and systems, *Proc. IEEE,* v. 88, n. 10, October 2000, pp. 1598–1612.
11. Jan M. Rabaey et al., PicoRadios for wireless sensor networks: The next challenge in ultra-low power design, *IEEE Int. Solid-State Circuits Conf. Digest of Technical Papers,* 2002, v. 1, pp. 200—202; v. 2, pp. 156—157, 444–445.
12. Lizhi Charlie Zhong et al., An ultra-low power and distributed access protocol for broadband wireless sensor networks, *Networld+Interop: IEEE Broadband Wireless Summit,* Las Vegas, 2001. http://bwrc.eecs.berkeley.edu.
13. Frazer Bennett et al., Piconet: embedded mobile networking, *IEEE Pers. Commun.,* v. 4, n. 5, October 1997, pp. 8–15.
14. http://www.uk.research.att.com.
15. Gray Girling et al., The design and implementation of a low power ad hoc protocol stack, *Proc. IEEE Wireless Communication and Networking Conf.,* September 2000, pp. 282–288.
16. Gray Girling et al., The PEN low power protocol stack, *Proc. 9th IEEE In. Conf. on Computer Communication and Networks,* v. 3, October 2000, pp. 1521–1529.
17. Rabaey et al., ibid.
18. G. Asada et al., Wireless integrated network sensors: low power systems on a chip, *Proc. 24th European Solid-State Circuits Conf.,* 1998, pp. 9–16.
19. Andrew Y. Wang et al., Energy efficient modulation and MAC for asymmetric RF microsensor systems, *IEEE Intl. Symp. Low* Power *Electronics and Design,* 2001, pp. 106–111.
20. Eugene Shih et al., Physical layer driven protocol and algorithm design for energy-efficient wireless sensor networks, *Proc. MOBICOM,* 2001, pp. 272–287.
21. K. Kim and K. K. O, Characteristics of integrated dipole antennas on bulk, SOI, and SOS substrates for wireless communication, *Proc. IITC,* 1998, pp. 21–23.
22. J. B. Bates, D. Lubben, and N. J. Dudney, Thin-film Li-$LiMn_2O_4$ batteries, *IEEE AESS Syst. Mag.,* v. 10, n. 4, April 1995, pp. 30–32.
23. W. C. West et al., *Thin Film Li Ion Microbatteries for NASA Applications.* NTIS order number N20000109952. Springfield, VA: National Technical Information Service. 1999.
24. Nelson (Hou Man) Chong et al., Lithium batteries for powering sensor arrays, in M. A. Ryan et al., Eds., *Power Sources for the New Millennium.* Pennington, NJ: Electrochemical Society proceedings volume PV2000-22, October 2000, pp. 266–271.
25. Clark T.-C. Nguyen, Micromechanical circuits for communication transceivers, *Proc. IEEE Bipolar/BiCMOS Circuits and Technology Meeting,* 2000, pp. 142–149.
26. Yannis Tsividis, Continuous-time filters in telecommunications chips, *IEEE Commun.,* v. 39, n. 4, April 2001, pp. 132–137.

27. Peter G. M. Baltus and Ronald Dekker, Optimizing RF front ends for low power, *Proc. IEEE,* v. 88, n. 10, October 2000, pp. 1546–1559.
28. Mehmet Soyuer et al., Low-power multi-GHz and multi-Gb/s SiGe BiCMOS circuits, *Proc. IEEE,* v. 88, n. 10, October 2000, pp. 1572–1582.
29. Peter Smulders, Exploiting the 60 GHz band for local wireless multimedia access: prospects and future directions, *IEEE Commun.,* v. 40, n. 1, January 2002, pp. 140–147.
30. Thomas H. Lee and Simon Wong, CMOS RF integrated circuits at 5 GHz and beyond, *Proc. IEEE,* v. 88, n. 10, October 2000, pp. 1560–1571.
31. However, regulatory requirements for certain applications, such as the Medical Implant Communications Service for implantable devices, may require operation as low as 402 MHz. U.S. Code of Federal Regulations, 47 C.F.R. §§95.601–95.673. Washington, D.C.: U.S. Government Printing Office. 2001.
32. Pete Fowler, 5 GHz goes the distance for home networking, *IEEE Microwave Mag.,* v. 3, n. 3, September 2002, pp. 49–55.
33. Jon M. Peha, Wireless communications and coexistence for smart environments, *IEEE Pers. Commun.,* v. 7, n. 5, October 2000, pp. 66–68.
34. Ivan Howitt, WLAN and WPAN coexistence in UL band, *IEEE Trans. Veh. Tech.,* v. 50, n. 4, July 2001, pp. 1114–1124.
35. U.S. Federal Communications Commission, *First Report and Order,* FCC 02-48, 14 February 2002. Washington, D.C.: U.S. Government Printing Office.
36. S. Meninger et al., Vibration-to-electric energy conversion, *Proc. Int. Symp. Low Power Electronics and Design,* 1999, pp. 48–53.
37. S. Meninger et al., Vibration-to-electric energy conversion, *IEEE Trans. Very Large* Scale I*ntegration (VLSI) Systems,* v. 9, n. 1, February 2001, pp. 64–76.
38. J. F. Freiman, Portable computer power sources, *Proc. Ninth Annu. Battery Conf. on Applications and Advances,* 1994, pp. 152–158.
39. S. Okazaki, S. Takahashi, and S. Higuchi, Influence of rest time in an intermittent discharge capacity test on the resulting performance of manganese-zinc and alkaline-manganese dry batteries, *Prog. in Batteries & Solar Cells,* 1987, v. 6, pp. 106–109.
40. Rodney M. LaFollette, Design and performance of high specific power, pulsed discharge, bipolar lead acid batteries, *10th Annu. Battery Conf. on Applications and Advances,* 1995, pp. 43–47.
41. E. J. Podlaha and H. Y. Chen, Modeling of cylindrical alkaline cells: VI variable discharge conditions, *J. Electrochem. Soc.,* v. 141, n. 1, January 1994, pp. 28–35.
42. Thomas F. Fuller, Marc Doyle, and John Newman, Relaxation phenomena in lithium-ion-insertion Cells, *J. Electrochem. Soc.,* v. 141, n. 4, April 1994, pp. 982–990.
43. Mark J. Isaacson, Frank R. McLarnon, and Elton J. Cairns, Current density and ZnO precipitation-dissolution distributions in Zn-ZnO porous electrodes and their effect on material redistribution: a two-dimensional mathematical model, *J. Electrochem. Soc.,* v. 137, n. 7, July 1990, pp. 2014–2021.
44. Richard Pollard and John Newman, Mathematical modeling of the lithium-aluminum, iron sulfide battery II: the influence of relaxation time on the charging characteristics, *J. Electrochem. Soc.,* v. 128, n. 3, March 1981, pp. 503–507.
45. C. F. Chiasserini and R. R. Rao, A model for battery pulsed discharge with recovery effect, *Proc. Wireless Commun. Networking Conf.,* 1999, v. 2, pp. 636–639.
46. C. F. Chiasserini and R. R. Rao, Routing protocols to maximize battery efficiency, *Proc. MILCOM,* 2000, v. 1, pp. 496–500.
47. C. F. Chiasserini and R. R. Rao, Stochastic battery discharge in portable communication devices, *15th Annual Battery Conf. on Applications and Advances,* 2000, pp. 27–32.
48. C. F. Chiasserini and R. R. Rao, Improving battery performance by using traffic shaping techniques, *IEEE J. Selected Areas in Commun.,* v. 19, n. 7, July 2001, pp. 1385–1394.
49. Supplied by Motorola.
50. Shih et al., ibid.

51. Wang et al., ibid.
52. Bernard Sklar, *Digital Communications: Fundamentals and Applications.* Englewood Cliffs, NJ: PTR Prentice Hall. 1988.
53. Shih et al., ibid.
54. Wang et al., ibid.
55. Jose A., Gutierrez et al., IEEE 802.15.4: A developing standard for low-power, low-cost wireless personal area networks, *IEEE Network,* v. 15, n. 5, September/October 2001, pp. 12–19.
56. U.S. Code of Federal Regulations, 47 C.F.R. § 15.247. Washington, D.C.: U.S. Government Printing Office. 2001.
57. U.S. Federal Communications Commission, *Further Notice of Proposed Rulemaking and Order,* FCC 01-158, 11 May 2001. Washington, D.C.: U.S. Government Printing Office.
58. U.S. Federal Communications Commission, *Second Report and Order,* FCC 02-151, 30 May 2002. Washington, D.C.: U.S. Government Printing Office.
59. European Telecommunication Standards Institute, Electromagnetic Compatibility and Radio Spectrum Matters (ERM); Wideband Transmission Systems; Data Transmission Equipment Operating in the 2,4 GHz ISM Band and Using Spread Spectrum Modulation Techniques. Document EN 300-328. Sophia-Antipolis, France: European Telecommunication Standards Institute. 2001.
60. Leon W. Couch II, *Digital and Analog Communication Systems,* 5th ed. Upper Saddle River, NJ: Prentice Hall. 1997.
61. The characteristic, or generating, polynomial is a compact way of identifying a particular PN sequence. For a detailed discussion, see Jhong Sam Lee and Leonard E. Miller, *CDMA Systems Engineering Handbook.* Boston: Artech House. 1998.
62. Isao Okazaki and Takaaki Hasegawa, Spread spectrum pulse position modulation — a simple approach for Shannon's limit, *Proc. ICCS/ISITA,* 1992, v. 1, pp. 300–304.
63. Isao Okazaki and Takaaki Hasegawa, Spread spectrum pulse position modulation and its asynchronous CDMA performance — a simple approach for Shannon's limit, *Proc. IEEE Sec. Intl. Symp. Spread Spectrum Techniques and Applications,* 1992, pp. 325–328.
64. Bernard Sklar, *Digital Communications: Fundamentals and Applications.* Englewood Cliffs, NJ: PTR Prentice Hall. 1988.
65. The equality

$$P_B(k) = \frac{M}{2(M-1)} \sum_{m=1}^{M-1} (-1)^{m+1} \frac{1}{m+1} C_m^{M-1} \exp\left(-\frac{mk}{m+1}\left(\frac{E_b}{N_0}\right)\right)$$

may be derived from Marvin K. Simon, Sami M. Hinedi, and William C. Lindsey, *Digital Communication Techniques: Signal Design and Detection.* Englewood Cliffs, NJ: PTR Prentice Hall. 1995. p. 325.
66. Bob O'Hara and Al Petrick, *The IEEE 802.11 Handbook: A Designer's Companion.* New York: IEEE Press. 1999.

Chapter 4
The Data Link Layer

4.1 INTRODUCTION[1]

Recent technology advances have made it conceivable to place wireless sensor networks in many applications. The wireless nodes of these networks will be comprised of a transducer (sensor or actuator), communications circuitry, and behavior logic. These nodes will be embedded in ceiling tiles, in factory equipment, in farmland, and on the battlefield, and will locate things, sense danger, and control the environment with minimal human effort. Crucial to the success of these ubiquitous networks is the availability of small, lightweight, low-cost nodes. Even more important, the nodes must consume ultra-low power to eliminate frequent battery replacement.[2]

To reduce the power consumption of these devices, both the operation and standby power consumption must be minimized; also, as described in Chapter 3, because the operation power consumption is greater than the standby power consumption, the communication time or time the communication circuits are active must be minimized. That is, the communication duty cycle must be reduced to a minimum.[3] For an asynchronous, multihop network (one in which no single node can serve as a global, centralized time reference), however, an ultra-low duty cycle makes it difficult for the wireless devices to discover and synchronize with each other, because they are so rarely active.

Low-cost crystal, ceramic, and on-chip Micro Electro-Mechanical System (MEMS) resonators[4] are regarded as key enabling technologies for ultra-low-cost wireless devices. The issue with these technologies is their relatively poor frequency stability, which compounds the device synchronization problem for ad hoc networks employing conventional time-division duplex (TDD) or time-division multiple access (TDMA) methods. Therefore, if the TDD beacon (or frame) period is nominally T_{beacon} seconds, and the timebase stability of each node is ε ppm, a node must begin every receiving period at least $2\varepsilon T_{beacon}$ seconds prior to the nominal reception time to ensure reception of the beacon (because both transmitter and receiver time bases may vary). Further, in the worst-case scenario, reception of the beacon may not begin until $2\varepsilon T_{beacon}$ seconds after the nominal reception time, so the receiver could stay active until that time, waiting for